

Modelling and Simulations on Current Collapse in AlGaN/GaN Power HEMTs

Huolin Huang, Yung C. Liang*, Ganesh S. Samudra, Yuling Li and Yee-Chia Yeo

Department of Electrical and Computer Engineering

National University of Singapore

Kent Ridge Crescent, Singapore 119 260

*contact author e-mail: chii (at) nus.edu.sg

Abstract— The influences of the trapped electron charges caused by high-voltage stress during pulse switching in AlGaN/GaN power HEMT devices resulting at a higher on-state resistance, known as the current collapse phenomena, are modelled, analysed by Sentaurus TCAD simulations, and verified with the laboratory measurement data. The quantitative relationships between the electric field and trapped electron densities can be determined using the detailed physic model described in this paper. Simulation verification shows a good match on current collapse characteristics in comparison with the measurement data.

Keywords - AlGaN/GaN HEMT, Current Collapse

I. INTRODUCTION

AlGaN/GaN high electron mobility transistors (HEMTs) have drawn great interest for high power and high frequency applications owing to its outstanding material advantages such as large critical electric field, high electron saturation velocity, and high-density two dimensional electron gas (2DEG) at the hetero interface. Although much progress has been achieved in AlGaN/GaN HEMTs with the innovation of the device structures and the development of the growth techniques of GaN-based materials, there are still important issues, such as low threshold voltage for normally-off device, current collapse, and self-heating effects, which need to be addressed. Among them, current collapse is very critical as it limits the output power and the switching characteristics of the power GaN devices when used in power electronic switching [1], [2].

Usually, current collapse phenomenon can be addressed by the “virtual gate” theory [3], where the electrons originated from the gate electrode are trapped at the surface defects near the gate at drain side under a large surface electric field during off-state. When the device is turned on, the trapped electrons cannot be removed in time and the induced field will deplete the 2DEG, acting like a gate extension but with a negative potential. Thus the increase of the on-resistance in this process results in the current collapse phenomenon. The current collapse phenomenon has been studied by many groups. Various approaches such as passivation of semiconductor surface and moderation of surface field were employed to suppress current collapse. It is thus necessary to inspect the inherent mechanism of the current collapse in detail, especially how the electric field affects the distribution of the trapped electrons near the gate and the corresponding relationship

between the number of the trapped electrons and the increase of the on-resistance.

Numerical simulations provide key insights into the electric behaviours and degradation mechanism of the power devices under current collapse. In this paper, the influences of the field induced trap charges under the current collapse conditions are investigated and simulated by Sentaurus TCAD [4]. Material parameters employed in the simulation, such as 2DEG density, electron mobility, and electron saturation velocity, are first calibrated by benchmarking I_d - V_d and I_d - V_g characteristics of HEMT devices under zero stress by laboratory measurement. The threshold voltage is primarily determined by the gate metal work function and 2DEG concentration. The on-state resistance is determined by 2DEG concentration and electron mobility, while on-state saturation current is determined by the electron saturation velocity. The device was then applied voltage stress and its current collapse effect on the on-state resistance change was measured by using the Agilent B1505A semiconductor device analyser. Verification was made between the simulation and measurement data to confirm the proposed model validity.

II. MODEL PHYSICS

A. The Trapped Charges

GaN epitaxy is known to have a high density of defects and dislocations due to lack of a native substrate. It is believed that a large number of donor-like traps, located at the top surface of AlGaN, act as a source of influence on 2DEG conductivity in AlGaN/GaN heterostructures while they also have an important impact on the characteristics of the GaN power devices such as current collapse [5]. Those deep donors, e.g. energy level at 0.37 eV below the conduction band, are assumed to be ionized completely [6]. The positive charges from the ionized donors will compensate the negative surface polarization charges which makes the surface electric field rather uniform. Therefore, the density of background electron and hole at the surface is much lower compared with the donor trap density. Under the off-state operation, electrons from the gate will get through the metal/semiconductor interface by the tunnelling and/or thermal emission process because of high electric field at the gate corner facing drain-side. The electrons can be temporally trapped in the ionized surface donor, causing the drain current to become much lower. The excess electrons then

This work received funding support from A*STAR Singapore under the GaN-on-Si TSRP Grant number 1021690127.

escape slowly after the device is turned on at lower drain voltage. This will then restore the surface charge state.

Besides the trapped charges on the top surface, there are also those at the AlGaIn/GaN interface, which is very close to the 2DEG channel. Although the amount of charges at the interface is relatively smaller than that existing on the top surface, their influence can be equally or more significant for its proximity to the 2DEG channel. Fig.1 shows the effect of these trapped charges influencing the device on-state resistance. The simulations were done with the parameters of 5.1 eV, 0.4, 1700 cm²/Vs, and 7.2×10⁶ cm/s set for gate metal work function, relaxation degree of the strained AlGaIn barrier layer, electron mobility, and electron saturation velocity in the simulation, respectively. As the electron trapping phenomena is strongly affected by the electric field [7], the distribution of the effective horizontal field within the 1.5 μm range provides a reliable basis for the surface trap region for devices without the surface field plates.

In this paper, the surface trap charges are modelled with much details. Trap charges near the 2DEG and substrate interfaces will be modelled in future work.

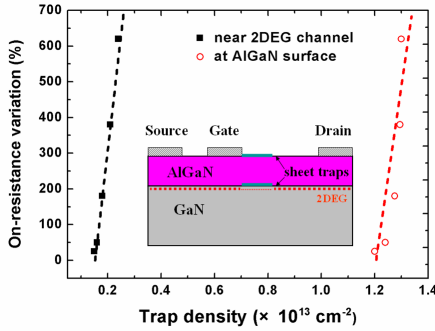


Fig. 1: On-state resistance variation as a function of the trapped electron density. Traps are set at the AlGaIn surface and just above the 2DEG channel, as shown in the schematic. The trap region length is set at 0.2 μm to demonstrate the effects. The dashed lines are best linear fits.

B. Modelling Process

1) Off-state stress process

The dynamics of electron trapping and emission on the AlGaIn surface is governed by the following equation:

$$\frac{\partial N_R}{\partial t} = C_{n,D} N_D^+ n - \frac{N_D - N_D^+}{\tau_E} \quad (1)$$

where $N_R = N_D - N_D^+$ is the density of trapped electrons in recombination with the ionized donors, N_D is the total donor density, and N_D^+ is the remaining ionized donor density.

N_R , N_D and N_D^+ are variables related with time t . It is reasonable to assume that the donor traps are fully ionized at room temperature when considering the trap energy level and strong polarization electric field at the AlGaIn surface. Therefore, $N_D^+ = N_D$ at time $t = 0$ just before the off-state

stress starts. In Eq. (1), $C_{n,D}$ determines the electron trapping time, $\tau_R = 1/(C_{n,D} N_D^+)$ where $C_{n,D}$ is a function of both electric field and free electron density. n is the excess electron density at the AlGaIn surface injected from gate metal which is much higher than the background electron density n_0 . τ_R and τ_E are the life time of electron trapping (capture) and emission (generation).

Combined with the boundary condition: $N_D^+ = N_D$ at $t = 0$. The following expressions can be derived.

$$N_D^+ = \frac{C_{n,D} N_D n \tau_E}{1 + C_{n,D} N_D n \tau_E} e^{-(C_{n,D} n \tau_E)^{-1} t} + \frac{N_D}{1 + C_{n,D} n \tau_E} \quad (2)$$

Or

$$N_R = -\frac{C_{n,D} N_D n \tau_E}{1 + C_{n,D} N_D n \tau_E} e^{-(C_{n,D} n \tau_E)^{-1} t} + \frac{C_{n,D} N_D n \tau_E}{1 + C_{n,D} n \tau_E} \quad (3)$$

Under steady state, i.e. $t \gg \tau_E$ and τ_R , we obtain

$$N_R = \frac{\tau_E}{\tau_R} n \left/ 1 + \frac{\tau_E}{N_D \tau_R} n \right. \quad (4)$$

The usage of the diffusion-recombination model gives a possible solution to describe the distribution of excess electron density $n(x)$ along the AlGaIn surface toward the drain side. Note that $n(x) \approx \Delta n \gg n_0$. The steady diffusion equation is shown as below.

$$D_n \frac{d^2 n(x)}{dx^2} = \frac{n(x)}{\tau_R} \quad (5)$$

Combined with the boundary condition: $n(x) = n(0)$ at $x = 0$ and $n(x) = n_0 \ll n(0)$ at $x \gg L_n$, we can obtain the excess electron density distribution as shown below.

$$n(x) = n(0) e^{-\frac{x}{L_n}} + n_0 \quad (6)$$

where $L_n = \sqrt{D_n \tau_R}$ is the electron diffusion length, and D_n is the electron diffusion coefficient. Thus, it is possible to get the final trapped electron charge distribution with the position x as a function.

$$N_R(x) = \frac{\tau_E}{\tau_R} \left[n(0) e^{-\frac{x}{L_n}} + n_0 \right] \left/ 1 + \frac{\tau_E}{N_D \tau_R} \left[n(0) e^{-\frac{x}{L_n}} + n_0 \right] \right. \quad (7)$$

The discussions till now are based on the assumption of constant $C_{n,D}$ and N_D^+ which in reality are related with the distribution of surface electric field and surface excess electron density. Here we proceed to make possible corrections to improve the model.

Considering the relationship, $\tau_R = 1/(C_{n,D} N_D^+)$, it is necessarily useful to amend τ_R for correction. The AlGaIn surface near the gate region facing drain side can be divided into two segments, namely, high field segment I and lower field segment II. For high field segment, $C_{n,D}$ is much lower as very few electrons are trapped. τ_R is large but decreases quickly. For low field segment II, $C_{n,D}$ increases and then be kept nearly

constant. So τ_R is treated as a small constant in this segment for simplicity. The relationship is shown in Fig. 2.

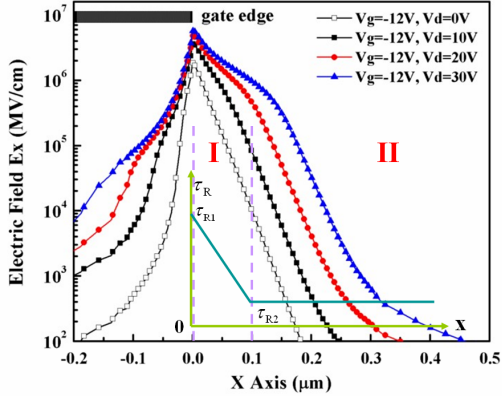


Fig. 2. Distribution plots of horizontal electric field at AlGaIn surface near the gate region facing drain side under different stress voltage. High horizontal field is present at 0.1 μm in range near the gate edge into the drain.

The basic parameters, τ_E , τ_R and L_n are shown as below.

$$\tau_R = \frac{1}{\sigma_{n,R} v_n N_D} e^{\frac{E_C - E_D}{kT}} \quad \text{and} \quad \tau_E = \frac{1}{\sigma_{n,E} v_n N_C} e^{\frac{E_C - E_D}{kT}} \quad (8, 9)$$

$$L_n = \sqrt{\frac{kT}{q}} \mu_n \tau_R \quad (10)$$

The positive charges from the ionized donors at the AlGaIn surface, $N_D = 2.5 \times 10^{20} \text{ cm}^{-3}$ and $n_0 = 1.0 \times 10^{10} \text{ cm}^{-3}$ are used in the calculation. The reported electron capture cross section for the deep donors is $10^{-13} \sim 10^{-15} \text{ cm}^2$ [8], here $\sigma_{n,R} = 1.0 \times 10^{-13} \text{ cm}^2$ is employed. Then using $\sigma_{n,E} = 1.2 \times 10^{-16} \text{ cm}^2$, $v_n = 6 \times 10^6 \text{ cm} \cdot \text{s}^{-1}$, $E_D = E_C - 0.37 \text{ eV}$, $N_C = 2.2 \times 10^{18} \text{ cm}^{-3}$ [6], and $\mu_n = 100 \text{ cm}^2/\text{Vs}$ [9], $\tau_{R2} = 1.0 \times 10^{-8} \text{ s}$ and $\tau_E = 9.6 \times 10^{-4} \text{ s}$ are found. τ_{R1} is defined as 10 times of τ_{R2} when considering the average field at region I is at least 2 orders of magnitude larger than that in region II. $n(0)$, closely related with the peak field, is obtained from the simulation fitting for $N_R(x)$ distribution. Fig. 3 shows the 2-D density of trapped electrons and excess mobile electrons when considering 1 nm-thickness AlGaIn surface layer. The inset shows the best linear fits between the trapped and excess electron sheet density and the average field at the gate corner.

2) On-state recovery process

When the device is turned on, the electric field at the AlGaIn surface is much reduced which results in the fall-off of excess carrier injection. The recombination process continues till the excess electron density is reduced to the background level. This process occurs as the initial phase of the current collapse, and the total amount of the negative charge, i.e. the sum of excess electrons and the trapped electrons, remains

unchanged. After the initial phase, the electron emission from the trapped state will become the dominant behaviour in the on-state recovery process. The process can be described as in (11).

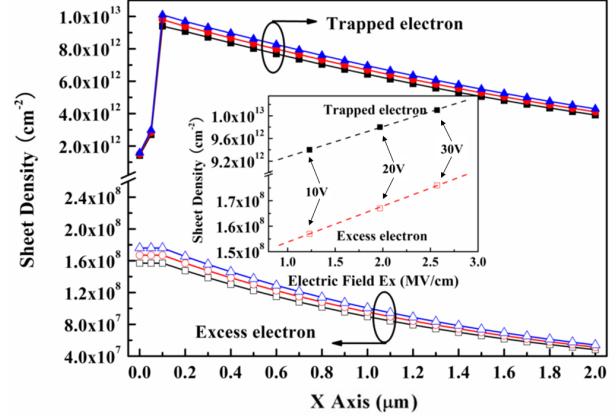


Fig. 3. The sheet density variation of trapped electron and excess electron with the position x under stress voltage 10 V (square point), 20 V (round point), and 30 V (triangle point). The inserted portion shows the peak values of N_R and n .

$$\frac{\partial N_R(x,t)}{\partial t} = -\frac{N_R(x,t)}{\tau_E'} \quad (11)$$

where $N_R(0)$ is the density of the trapped electrons at the beginning. τ_E' is the life time of electron emission in recovery process. Combined with the boundary condition, $N_R(x,t=0) = N_R(x)$ and $N_R(x,t=\infty) = 0$ at $t \gg \tau_E'$, we can obtain the function of the trapped electrons with time t as shown in (12).

$$N_R(x,t) = N_R(x) e^{-\frac{t}{\tau_E'}} \quad (12)$$

The Poole-Frenke emission mechanism states that electric field will influence on the activation energy for electron emission (0.2 - 0.25 eV smaller at 1 MV/cm), which results at 10^3 ratio in generation life time change [7]. A higher generation lifetime of $\tau_E' = 2 \text{ s}$ is set here for the recovery phase.

III. MODEL VERIFICATION

The device structure is show in Fig. 4(a) with $L_g = 2 \mu\text{m}$, $L_{gs} = 5 \mu\text{m}$, $L_{gd} = 5 \mu\text{m}$, and $W_g = 100 \mu\text{m}$. Al_2O_3 insulator thickness is 15nm. The device is not passivated which is helpful to observe and investigate current collapse phenomena. Sentaurus TCAD is used to simulate the I-V characteristics of the HEMT device. The device parameters are calibrated first by comparing with the measurement data, followed by the current collapse studies. The parameters used in the simulation are shown in Table I.

For the current collapse simulation, it is found that the current reduction is significant when the trapped-electron density is greater than $5.0 \times 10^{12} \text{ cm}^{-2}$, where two regions,

0.4 μm (at $x > 0.1 \mu\text{m}$) wide and 0.8 μm (at $x > 0.5 \mu\text{m}$) are set with proper trapped charges. At the off-state, a gate bias of -12 V is applied with a drain stress bias ranging from 10 to 30 V for 2 seconds. After removing the stress bias, the on-state drain current is measured.

Table I. Parameters used in the simulation

Gate metal workfunction	4.6 eV
2DEG density	$8.0 \times 10^{12} \text{ cm}^{-2}$
2DEG Electron mobility	$280 \text{ cm}^2/(\text{vs})$
Electron saturation velocity	$2.25 \times 10^6 \text{ cm/s}$

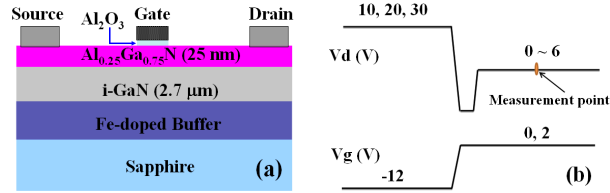


Fig. 4. (a) Device structure of AlGaIn/GaN HEMT and (b) timings in current collapse measurement. The off-state stress time is kept at 2s and the measurement point is 0.51s after removing the stress bias. Fig. 5 shows a good match between the measurement and simulation drain current data. And, Fig. 6 shows the entire drain current recovery process as a function of time.

IV. CONCLUSIONS

The physical model for AlGaIn/GaN HEMT devices is built up to simulate current collapse phenomena and is verified by the experimental measurement. The results are in agreement with the trapped charges appropriately placed. The quantitative relationships between the electric field and trapped-electron densities and distribution can be determined using the detailed physic model described in this paper.

REFERENCES

- [1] K. Ohi and T. Hashizume, "Reduction of current collapse in the multi-mesa-channel AlGaIn/GaN HEMT," *Phys. Status Solidi C*, vol. 9, no. 3-4, pp. 898-902, March 2012.
- [2] K. Makiyama, T. Ohki, N. Okamoto, et al., "High-power GaN-HEMT with low current collapse for millimeter-wave amplifier," *Phys. Status Solidi C*, vol. 8, no. 7-8, pp. 2442-2444, June 2011.
- [3] R. Vetury, N. Q. Zhang, S. Keller, and U. K. Mishra, "The impact of surface states on the DC and RF characteristics of AlGaIn/GaN HFETs," *IEEE Trans. Electron Devices*, vol. 48, no. 3, pp. 560-566, March 2001.
- [4] Synopsys Inc., "Sentaurus Device User Guide, Version D-2010.03," March 2010.
- [5] B. Jogai, "Influence of surface states on the two-dimensional electron gas in AlGaIn/GaN heterojunction field-effect transistors," *J. Appl. Phys.*, vol. 93, no. 3, pp. 1631-1635, February 2003.
- [6] H. Hasegawa, T. Inagaki, S. Ootomo, and T. Hashizume, "Mechnisms of current collapse and gate leakage currents in AlGaIn/GaN heterostructure field effect transistors," *J. Vac. Sci. Technol. B*, vol. 21, no. 4, pp.1844-1855, July/August 2003.

- [7] O. Mitrofanov and M. Manfra, "Poole-Frenkel electron emission from the traps in AlGaIn/GaN transistors," *J. Appl. Phys.*, vol. 95, no. 11, pp. 6414-6419, June 2004.
- [8] K. Horio, K. Yonemoto, H. Takayanagi, and H. Nakano, "Physics-based simulation of buffer-trapping effects on slow current transients and current collapse in GaN field effect transistors," *J. Appl. Phys.*, vol. 98, no. 12, p. 124502, December 2005.
- [9] V. O. Turin, "A modified transferred-electron high-field mobility model for GaN devices simulation," *Solid-State Electron*, vol. 49, no. 10, pp. 1678-1682, October 2005.

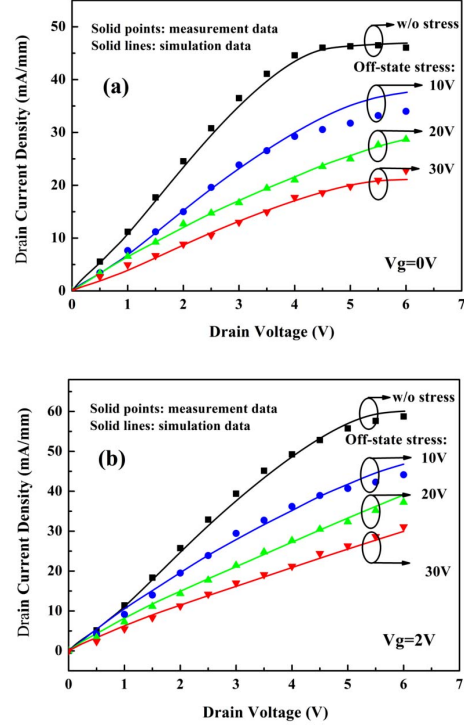


Fig. 5. Comparison of simulated I_d - V_d characteristics with the measurement data after different off-state stress bias. Trapped charge density @10V: 7.3×10^{12} , $5.6 \times 10^{12} \text{ cm}^{-2}$; @20V: 7.6×10^{12} , $6.2 \times 10^{12} \text{ cm}^{-2}$; @30V: 7.8×10^{12} , $6.6 \times 10^{12} \text{ cm}^{-2}$.

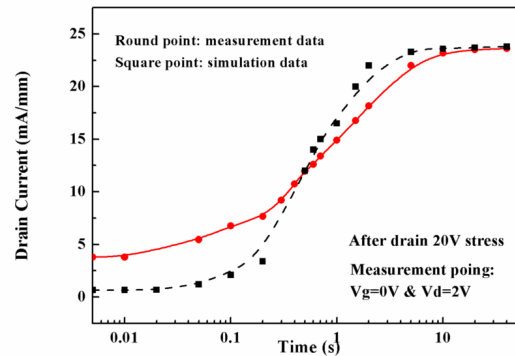


Fig. 6. Drain current recovery as a function of time